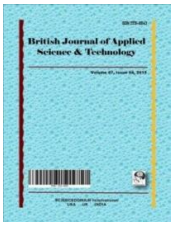

British Journal of Applied Science & Technology
13(6): 1-21, 2016, Article no.BJAST.19082
ISSN: 2231-0843, NLM ID: 101664541

SCIENCEDOMAIN *international*
www.sciencedomain.org

Technologies in Texture Analysis – A Review

Tuhin Utsab Paul[1*], Pranavesh Banerjee[1], Anannya Mukherjee[1] and Samir Kr. Bandhyopadhyay[2]

[1]Department of ECE, Institute of Engineering and Management, Kolkata, India.
[2]Department of CSE, University of Calcutta, Kolkata, India.

Authors' contributions

This work was carried out in collaboration between all authors. Author TUP designed the study and wrote the first draft of the manuscript. Authors PB and AM managed literature searches and comparative analysis. Authors TUP and SKB managed the literature searches and editing of the manuscript. All authors read and approved the final manuscript.

Article Information

DOI: 10.9734/BJAST/2016/19082
Editor(s):
(1) Wei Wu, Dalian University of Technology, China.
(2) Meng Ma, Anhui University, Hefei, Anhui, China, Icahn Institute for Genomics and Multiscale Biology, Icahn School of Medicine at Mount Sinai, New York, USA.
Reviewers:
(1) Anonymous, Army Institute of Technology, Pune, India.
(2) Jia-Shing Sheu, National Taipei University of Education, Taipei, Taiwan.
(3) Anonymous, University of Nevada Las Vegas, Nevada.
(4) Anonymous, University of science and Technology Houari Boumediene, Algiers, Algeria.
(5) S.Selva Nidhyananthan, Mepco Schlenk Engineering College, India.
(6) Zhi-Yong Bai, Beijing Forestry University, China.
Complete Peer review History: http://sciencedomain.org/review-history/12759

Review Article

Received 24th May 2015
Accepted 24th November 2015
Published 22nd December 2015

ABSTRACT

Texture analysis is one of the promising field of digital image processing. The main target of texture analysis or recognition is to understand, process and model texture, and ultimately simulate human visual learning process using different computer technologies, which are generally done through different texture analysis methods like spatial method, structural method, statistical method. In this paper, we had analyzed the different problem areas in this field, to highlight the gap or shortcomings in technology and the possible ways to bridge those gaps in technology.

Keywords: Image processing; image segmentation; texture recognition; color image processing, appearance based modeling; bidirectional texture; pulse function; pulse image processing; BTF; neural networks.

**Corresponding author: E-mail: tuhin.paul@iemcal.com;*

1. INTRODUCTION

One of the major issues faced in the field of image processing and computer vision is texture analysis or recognition, which has been an active research topic since almost three decades. Texture analysis was widely applied in various areas like remote sensing, object recognition, mobile robot navigation, estimation of 3D surface area from 2D images, contour based image retrieval and many more. Multiple algorithms or mathematical modeling methods have been proposed for texture analysis, and they can be classified into three major categories: statistical methods, model based methods and structural methods. Each method has its own merits and demerits.

This paper provides a comprehensive review about different technologies in texture analysis field. The paper is organized as follows –Section II provides background information about the texture analysis and its methods, texture spectrum and texture classification using the fractal method; Section III discusses the different conventional texture recognition technologies .Existing research work and their corresponding results, merits and demerits are discussed in Section IV. Section V discusses on the possible ways to overcome the gap or shortcomings in technology and the future expected work in the field of texture analysis.

2. TEXTURE ANALYSIS

Humans perceive scenes that have variation of intensity and color, which have the repeated patterns called the texture. Now what is a texture? In a very basic way a texture is an ensemble of repeated sub patterns that follows a set of well defined placement rules. These sub patterns comprised of fundamental units which are called primitives.

Texture analysis refers to the characterization of regions in an image by their texture content. Texture analysis is an attempt to quantify intuitive qualities described by roughness, smoothness, silkiness, or bumpiness that is a function of the spatial variation in pixel intensities. The roughness or bumpiness refers to variations in the intensity values, or gray levels. Texture analysis has a wide spread scope.

Texture analysis is used in a variety of applications, including remote sensing, automated inspection, and medical image processing.

Texture analysis can be used to find the texture boundaries which are called texture segmentation. Texture analysis is helpful when objects in an image are more characterized by their texture than by intensity. Texture analysis has a distinct application in the field of applied crystallography where the crystal structure, stress, strain and crystal size determination is done.

In [1], the various attributes and the utilities of the texture are explained in brief. The classification of the object pattern becomes easy if we can identify the texture. The attributes of the texture is defined as coarseness homogeneity, orientatition and the spatial relationship between image intensities or tones is determined [1]. Based on the attributes, texture is broadly classified as micro-texture and macro-texture. Both micro-texture and macro-texture are composed of primitive elements with specific shapes, sizes and placements. Two important attributes of such textures are coarseness and directionality. Coarseness relates to the size of the texture elements. If the primitive element size is large, then the texture is termed a coarse texture or macro texture and if the size is small the resultant texture is a fine or micro texture. Directionality corresponds to the orientation of the texture elements and to their spatial arrangement [1].

Based on feature selection, texture understanding method is classified as spatial methods, structural methods and statistical method. In spatial methods, a texture is modeled as a segmented region from which spatially compact and visually perceptual features such as the lines, edges, orientation, etc., are extracted over a larger area. The method looks for such repetitive perceptual features, and creates a vector of these perceptual features in the texture. In structural characterization, a texture is viewed as made up of many primitive textural elements, called ‘texel’, arranged according to some of the specific placement rules. In statistical methods a texture is defined as a random field and a statistical probability density function model is fitted to the spatial distribution of intensities in the texture. This methods measure the interactions of small number of pixels. A popular statistical tool for extracting second-order texture information from images is the gray level concurrence matrix [1]. To understand the

statistical correlation of different textures, a detailed understanding of the texture spectrum is necessary [2-4].

2.1 Texture Spectrum

Texture Spectrum is a statistical way of describing the different texture features which are present in an image [5-7]. In this method usually a texture unit represents the local texture information for a given pixel and its neighbourhood, and the global texture of an image is represented by the texture spectrum. A texture image is represented by a set of small units called as texture unit that usually represent or prove that local texture information for a good pixel and neighborhood of that pixel [8,9].

In Square Raster Digital image, a single pixel present in an image is surrounded by eight neighboring pixels. The local texture information for a particular pixel is then extracted from the neighboring pixel that represents the elements of 3 by 3 window sorrounding the pixel. Thus texture spectrum information from the eight neighborhood pixels that form a smallest unit. In neighborhood of 3 by 3 pixel. Let V= {Vo, V1….V8), a set denoting nine elements where Vi(i=0,1….8) represents the gray level of the ith element in the neighborhood where Vo denote the gray level of the central pixel.

TU (Texture Unit) of the pixel is obtained which is defined by a set containing element. TU= {e1, e2, e3….e8) where Ei (i= 1, 2…8).

Ei=0 where Vi<Vo, Ei=1 where Vi=Vo, Ei=2 where Vi>Vo. Here element Ei occupies the same position as the pixel i. Texture units are represented by the formulae NTU=3^(i-1) Ei where i=1,2….8 where NTU represent texture units. Each texture unit number describes the local texture aspect of a given pixel that describes the relative gray level relationship that exists between the central pixel and its neighborhood. Therefore texture spectrum is defined as the frequency distribution of all the texture unit (numbers) with the abscissa that represent the NTU and the coordinate frequency of its occurrence [10-12].

2.2 Texture Classification Using Fractals

The fractal properties of an image are based on and computed from the rate of the decrease of areas where an image is captured at a course of resolution n as the finer details present inside the area disappears when images are captured in lower resolution or scales.

Fractal properties are used for texture classification amongst various images and texture components.

2.2.1 Fractal lines and shapes

The estimated length L(S) is related to the fractal dimension d of the line by the formulae L(S)=Fexp^(1-d) where F=constant for a particular line type. The estimated length is the true distance between two points in case of the straight line. In case of the straight line the actual distance is exactly equal to the estimated distance and this fractal dimension is calculated from the slope of the line present in the textured image.

2.2.2 Fractals in texture classification

Each pixel in a textured image is considered as cuboids with its length and width equal to the pixel dimension and height equal to the pixel intensity. The total exposed surface indicated the surface area of the texture. The area is calculated at different integer ruler sizes L which is obtained by calculating different integer ruler sizes L by averaging adjacent pixels to generate a new image with pixel size L. Thus we inferred that A(L) is propositional to L(2-D) where D is the fractal dimension of the image. D can be calculated from the slope of A(L) versus L in logarithmic scale [13-16].

3. TEXTURE RECOGNITION TECHNIQUES

There are many techniques for identifying textures in different contexts, like active contour model, shape distortion and normalisation method, fourier based shape descriptor method, and region based shape descriptor method, which are discussed in brief below.

3.1 Active Cotour Model

Monochromatic image segmentation utilizes the basic properties of the gray level images to detect. Thresholding, region growing region splitting and merging are the ways in which segmentation can be performed. The limitation of this image segmentation is that it produces spurious edges, gaps, edge grouping, and complete reliance on the information contained in the local neighborhood of an image. Active

contour models on snakes proposed in [17-20] provide an approach to visual analysis. Snakes are contour model which are used to detect the boundary and shape of an object as well as to track a moving object in an image sequence .Snakes are used for edge and curve detection, segmentation, shape modeling and visual tracking. Basically snake is a parametric curve and its properties are specifies through a function which is called an energy functional.

3.2 Shape Distortion and Normalisation Method

Based on the camera placement there are four possible basic forms of planar object shape distortions-rotation, scaling, translation, and skewing. A good shape descriptor should not be affected to these distortions. So it is of prime importance to normalize the shape patterns in its original and various distorted forms, such as scaled, rotated, translated or skewed forms, so that they al1, more or less, resemble similar to each other. When an appropriate set of features are extracted only after such a normalization, shape classification yields much better accuracy. Considering shape normalization of a binary image f (s, y) in which f (s, y) = 1 indicates that (2,y) is an object pixel, otherwise it is a background pixel. Such a normalization algorithm to normalize the shapes, called shape compacting involves the following steps:

1. Computing the shape dispersion matrix M,
2. Aligning the coordinate axes with the eigen vectors of hl,
3. Rescaling the axes using the eigen values of hl.

3.3 Fourier Based Shape Descriptor Method

In this method firstly an object shape signature is computed. Then the discrete Fourier transform is computed on the shape signature. This signature is obtained from either the boundary points of the object or they are computed from the curvature and radii information of the boundary points. These points are captured at the interval of equal angles from the centroid. Now after computing the fourier transform on shape signature, fourier coefficients captures the general shape characteristic. Fourier descriptors that are computed are affected by the rotation and scaling of the image, so appropriate normalization of the boundary is required to make it a standard size and orientation. Fourier descriptors preserves all the attributes of the shape of an object.

3.4 Region Based Shape Descriptors

It takes in to account all the interior and boundary pixels of the shape. The prominent region of the shape descriptor is based on the moment. The moments are geometric moment, Hu's invariant moment, Zernike moments, Radial Chebyshev moments. Different types of moments are used for different moment based classification.

4. RECENT WORKS ON TEXTURE ANALYSIS

From the last two decades research has been going on in the field of texture recognition. Different texture recognition tools, methods, algorithms are used and are applied in a variety of areas starting from medical images to the satellite images. In this paper we have mainly concentrated on the skin texture recognition [21-23].

A prior work on the texture recognition of medical images using the Integrated Cortical Method [24] is proposed in 2004. Many of the texture recognition algorithms rely on the statistical analysis of image segments. In this paper a new approach is proposed which depends on pulse image spectra. The image texture is processed by a higher order network and cognitive pulsations are used to extract the image texture. Generally the various techniques which are frequently applied to a standard texture database for texture analysis are Auto-correlation method, co-occurrence method, edge frequency method, law's method, Run Length method, binary stack method, method of texture operators.

This paper represents a model that uses 'pulse image' generators to eventually determine the 'pulse spectrum' of each pixel. These spectra are then used to classify the pixels. Pulse images are generated from a single input image. Basically each pixel, which is also termed as neuron consists of a coupled oscillator consisting of an internal state (F) and a dynamic threshold. It is mathematically convenient to group the F's of all the pixels into a single 2D array, F. Similarly, the thresholds are also described as an array. The pulse images tend to isolate the segments, textures, and edges that are

contained in the input image. The pulse spectra of an image are indicative of the texture-contained therein. Therefore, a library of pulse spectra can be created and used to classify unknown spectra via simple matching of associative memories.

The method or the system is not perfect but still large segments of the image are classified correctly. To improve classification a more complex recognition scheme was employed. An improvement in recognition can be realized by employing an associative memory. The FAAM (fast analog associative memory) was employed here to recognize pulse spectrum from several training examples. It classifies each pixel as Yes (white), No (black), or Undecided (grey). Fig. 1 and Fig. 2 shows the results of the above algorithm.

A work on the bidirectional imaging and modeling of skin texture, [25] presents a method of skin imaging which is termed as the bidirectional imaging that captures significantly more properties of appearance than standard imaging. Specific protocols and methods like bidirectional texture function (BTF) are used to achieve the bidirectional imaging and used to create the Rutgers Skin Texture database (clinical components). Now using the skin texture database, computational surface modeling was used to perform automated skin texture classification using BTF.

In this paper, it is shown that a typical digital image does not contain sufficient information to mimic a real clinical visit. The salient features in a digital image are very dependent on imaging parameters like namely, camera and illumination direction. Therefore a single image cannot capture all the properties of skin appearance that may be important for diagnosis. In this method, a series of images is captured while varying the direction of the camera and light source, the salient features of skin texture are not discernible in a single image, but the bidirectional image set better captures the complete appearance. For computer assisted applications there are additional challenges beyond captures images. Computer assisted evaluation requires a computational representation based on directional images to extract useful quantitative information. This type of quantitative evaluation is a fundamental problem but bidirectional imaging gives a starting point.

A structure can be imaged computationally by applying a simple Lambertian shading model to the surface geometry. Specifically, the computed image having intensity I(x,y) is obtained from the local surface normal N(x,y) and the illumination direction L(x,y) from a vector equation given as

$$I(x,y) = N(x,y).L(x,y)$$

However, this model is oversimplified. The reflectance properties of the skin are vastly complex.

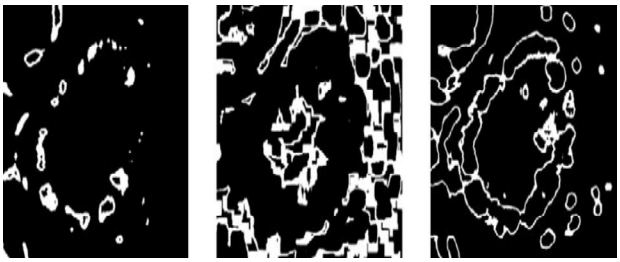

Fig. 1. Classification of pixels as epithelial nuclei, cytoplasm, or secretion [24]

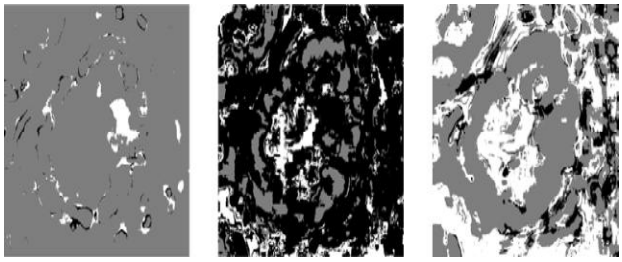

Fig. 2. Results from the use of an associative memory [24]

The typical imaging scenario employed by dermatologists in a clinical setting involves a regular digital camera positioned frontally to the surface of interest, illuminated by the ambient light available in a common clinical environment. No attempt is made to calibrate the viewing direction or the lighting conditions. To obtain bidirectional measurements, the illumination source and camera should be moved in positions corresponding to points sampling a hemisphere of possible directions. Bidirectional measurements can be quite difficult to obtain due to mechanical requirements of the setup. When the sample is nonplanar, nonrigid and not-fixed, as is the case for human skin, measurements are even more cumbersome.

In bidirectional imaging the main problem that is faced is to obtain bidirectional measurements, the illumination source and camera should be moved in positions corresponding to points sampling a hemisphere of possible directions. They presented two techniques in this paper to achieve bidirectional imaging.

Method 1: uses a light arc and a camera mounted on a tripod.
Method 2: uses a modified light arc and a camera manipulator that was also used for the face texture database [25].

These two methods are essentially the same because in both the camera and illumination are carefully controlled and a series of images is obtained. But bidirectional measurements are itself very difficult to obtain due to mechanical requirements of the setup. The only difference is that the equipment for method 2 allows more convenient positioning for facial imaging.

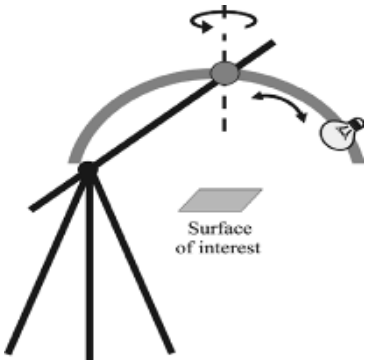

Fig. 3. The illumination setup for imaging method 1. [25] Various light poses are obtained by mounting the light source on a rotative arc. The setup allows scanning of horizontal surfaces

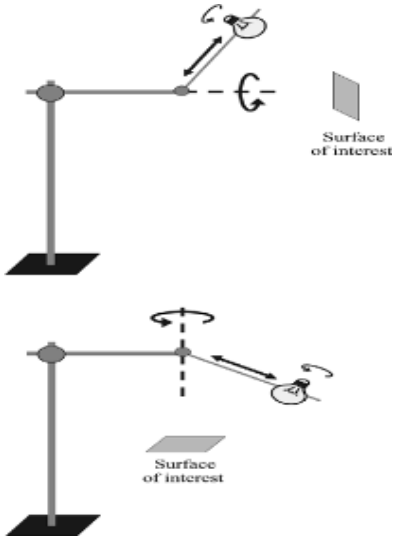

Fig. 4. Illumination setup for imaging method 2. Various light poses are obtained by mounting the light source on a rotative arc. The setup allows scanning of either vertical (top image) or horizontal surfaces (bottom image)

The recognition method consists of three main tasks: (1) creation of image texton library, (2) training, and (3) classification.

Many standard approaches in texture modeling characterize an image texture with a feature distribution. Models for bidirectional texture also need to account for changes in appearance with viewing and illumination direction. In this method, the distribution or histogram of features is a function of illumination and viewing direction. In this paper, each texture class is modeled using a collection of 'texton' histograms. The dimensionality of the histogram space is given by the cardinality of the image 'texton' library, which should be inclusive enough to represent a large range of textured surfaces.

A number of skin segmentation algorithm [26] relay on skin colour only, but this work relies on both skin color and texture features (features derived from GLCM). Feed forward neural network is used to classify input texture images to be skin or non-skin textures. The proposed skin texture recognition algorithm consists of three main tasks.

(1) Creation of the library of representative skin features,
(2) Neural Network Training, and
(3) Classification.

The library of skin texture is comprised of 300 images of skin textures of size 80X80 pixel. The library consisted of variety of skin types of different human races, different places of the human body and different lighting conditions.

Feed forward back propagation neural network with adaptable learning rate is used as shown in Fig. 5. The Neural network have 3 layer; an input layer (13 neuron), a hidden layer (50 neuron), and output layer (1 neuron). The input to the neural network is the feature vector and has 13 components these are the 4 texture feature and the three color moments for each color component (R G B), the NN has only one output as shown in Fig. 3 and Fig. 4.

The NN training process is done using skin and non-skin texture images from the image library. The output of the neural network assumed to be 1 for skin input image and -1 for non-skin input image. Matlab 7.0 was used to implement the system. SSE (sum square error) was the performance criterion.

It can be concluded from the Figs. 6, 7 and 8 that the system gave very encouraging results for both skin and non-skin inputs. The use texture and color feature enhanced the performance of the system and gave recognition accuracy of 96% in the generalization test. This accuracy proves that the texture features are very useful as recognition features for skins in addition to color features that are used in many applications. Images that are either taken under lighting conditions are very different from the lighting conditions under which that training set is taken, or they are not plane skin texture i.e. they contain 3D shadow. This is the limitations of this method.

The article classification of color images of dermatological ulcers [27], color image processing methods is presented for the analysis of images of dermatological lesions. In this paper the main aim is on the application of feature extraction and selection methods which is used for the classification and analysis of tissue composition of skin lesion or ulcers in terms of granulation (red), fibrin (yellow), necrotic (black), callous (white) and mixed tissue composition. For the feature extraction, each image is first manually segmented into 2 regions one into lesion and the background by an MACF. For each image the H component, saturation component, L*u*v color component and L*a*b color component is calculated. Based on the R, G, B, S, u*, v* a*, b* component the mean skew ness and kurtosis values are computed.

The next step is feature selection procedure. For the feature selection procedure, wrapper algorithm was used. The Wrapper algorithm generates candidate subsets of attributes and evaluates them by using a learning scheme. This process is repeated with each candidate set until the stopping criterion is reached. Cross validation is used to estimate the accuracy of the learning scheme for a given set of attributes. Cross validation is a sampling method for the analysis of the performance of a classifier that randomly divides the samples into r mutually exclusive partitions (folds) of approximately equal size of n/r samples, where n is the total number of available samples. For the classification method, the classifiers that are chosen to run the wrapper algorithm are naïve bayes, multilayer perception, decision tree, and the k-nearest neighbor classifier. The naive Bayes classifier calculates the probability of a sample which is used to generate a model with a decision rule

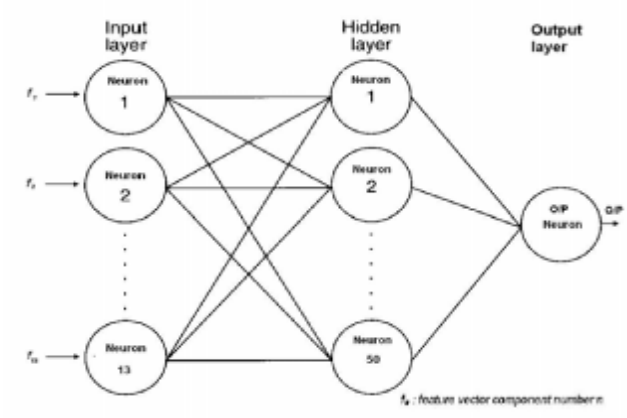

Fig. 5. Neural network structure [26]

that always provides a response indicating the class that has the highest probability after application of Bayes theorem. The MLP classifier consists of a set of nodes that constitute the input layer, one or more intermediate or hidden layers of computational nodes, and an output layer. The set of measurements to be classified is provided to the input layer and propagates forward, through the hidden layers toward the output layer, creating a computed value for classification. Decision trees employ a strategy of divide-and-conquer, decomposing a larger problem recursively into simpler sub problems. The KNN classifier finds the k nearest neighbors of the sample to be classified, typically by using a distance metric (usually the Euclidean distance) between the attributes of the sample to be classified and the attributes of all of the available samples with known classification. In this study, the k value used for the KNN classifier is 10. Fig. 9 shows the results.

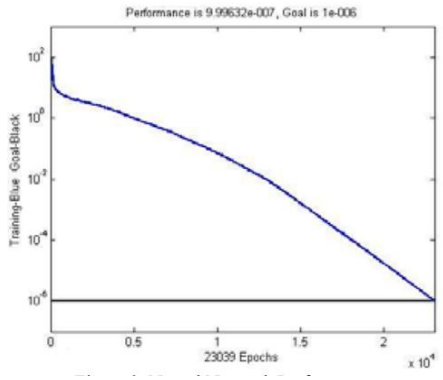

Fig. 6. Neural network performance [26]

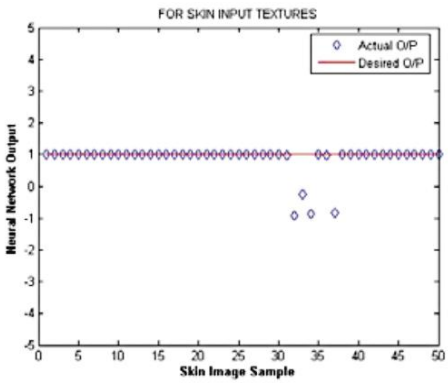

Fig. 7. Neural network generalization O/P for skin input images [26]

We analyzed the frequency of selection of each attribute in the twelve tests. An evaluation test was conducted with the classifiers used (naive Bayes, MLP, KNN, and decision trees) and the attributes selected once or more, twice or more, until eight times, which was the highest frequency obtained. The labeling of the images by the dermatologist was used in training and testing of the classifiers. The percentage of correctly classified images and the area under the receiver operating characteristic (ROC) curve were computed for comparative analysis. The ROC curve is obtained by plotting a graph of the sensitivity versus (1-specificity). The sensitivity of classification is the ratio of the true negatives to the number of negative samples. Then, the area under the curve (AUC) is calculated. A large AUC indicates good performance in classification. In summary, we can state that, based on the experiments conducted in this study, the best approach to the classification of color images of dermatological ulcers is the MLP classifier with the following features: homogeneity between the components a* and b*, contrast between the components a* and b*, entropy between a* and b*, and contrast between the components u* and v*. Fig. 10 and Fig. 11A shows the statistical evaluations of the method.

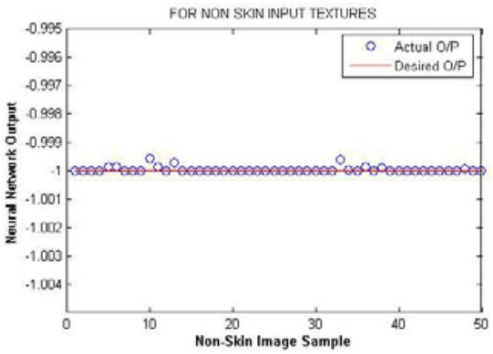

Fig. 8. Neural network generalization O/P for skin input images [26]

In the paper, Binary Tissue Classification on Wound Images with Neural Networks and Bayesian Classifiers [28] it is said that European Pressure Ulcer Advisory Panel (EPUAP) defines a pressure ulcer as an area of localized damage to the skin and underlying tissue caused by pressure, shear, friction, and/or a combination of these. The prevention, care, and treatment of pressure ulcer pathology involve high costs for health services and imply important consequences for the health of the population.

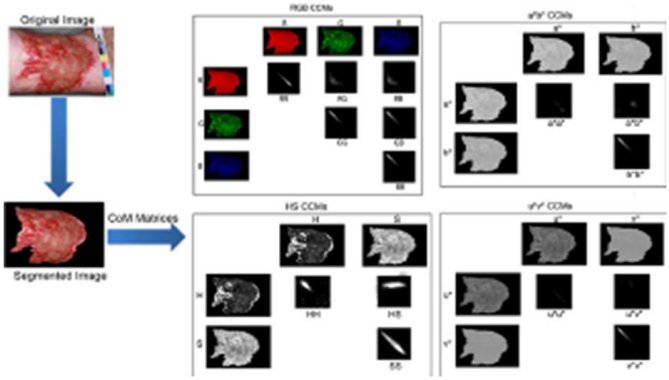

Fig. 9. Creation of CCMs for the analysis of texture in color images

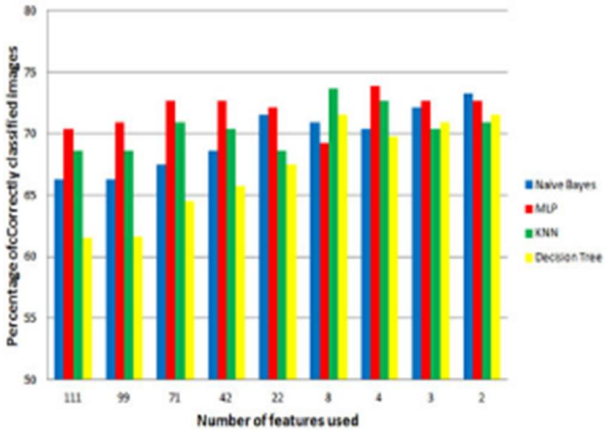

Fig. 10. Percentage of correctly classified images with each classifier using different thresholds on the frequency of selection of the attributes. The labels on the horizontal axis indicate the numbers of features in the various sets of features used, starting with all of the 111 features computed, the features selected once (99), twice (71), and so on to eight times (2)

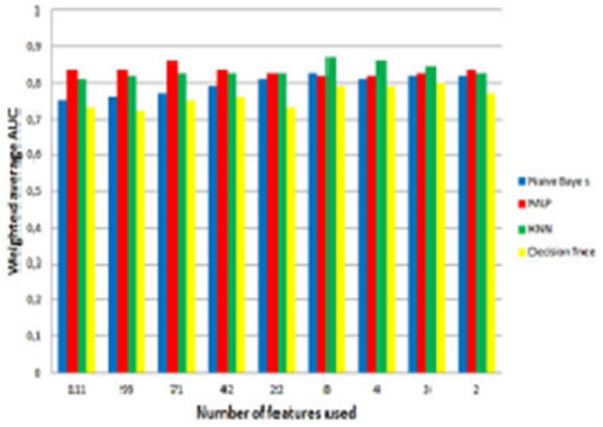

Fig. 11A. Weighted average AUC for each classifier using different thresholds on the frequency of selection of the attributes. The labels on the horizontal axis indicate the numbers of features in the various sets of features used, starting with all of the 111 features computed, the features selected once (99), twice (71), and so on to eight times (2)

Precise evaluation of pressure ulcers constitutes a crucial task in diagnosing, monitoring the evolution and decisions on care interventions and pharmacological treatments to be arranged for each particular case. Clinicians generally evaluate and register each pressure ulcer using standardized scales and indexes, which are based mainly on the visual inspection of the wound together with other relevant data about the patient's health-state. Nevertheless, visual inspection constitutes actually a very subjective and inaccurate way to deal with the accurate classification of tissues in this sort of wound.

The main objective of this paper is to design a computational approach to tissue recognition in pressure ulcer images. In order to accurately evaluate the wound state, pressure ulcer tissues have to be detected, segmented and finally measured.

This paper presents several image processing techniques and a hybrid approach based on neural networks and Bayesian classifiers to design an automatic procedure for effective region segmentation and identification of significant tissues in pressure ulcer color-digital images. Neural networks have shown high efficacy rates when applied to similar clinical problems such as melanoma diagnosis by digital dermoscopy. The proposed methodology includes:

1) Using image processing techniques such as filtering, kernel smoothing by the mean shift procedure, and region growing to segment the images;
2) Extracting significant color and texture features from these segmented regions;
3) Using statistical analysis to reduce the dimensionality of the feature space;
4) Training a set of supervised neural networks—multilayer perceptrons to classify the segmented regions as belonging to one of the different tissue categories proposed by the clinicians; and
5) Training a Bayesian classifier to form a Bayesian Committee Machine (BCM) which combines the predictions from the neural networks to improve the classification performance scores of the system.

Fig. 11B describes the overall process for region segmentation and tissue identification on pressure ulcer digital images. Clinicians took color photographs of pressure ulcers of patients with home-care assistance. One of the most critical concerns for effective tissue identification on wound images is the accurate segmentation of the specific regions present in the image. Pressure ulcers mostly have irregular shapes, vague boundaries, and very heterogeneous colorations. These conditions make precise automatic segmentation a nontrivial computational task, where traditional image processing techniques—such as histogram thresholding, border detection using masks, or watersheds—usually fail. Active contour modeling can give good solutions to the partial problem of skin/wound segmentation or wound-border detection, but has some limitations when it is applied to specific pressure ulcer images taken in environments where the lighting may be less than ideal. On the other hand, skin texture models could also be used to deal with the partial problem of separating skin from wound tissues, but the heterogeneous and imprecise nature of the images is again a strong handicap for these methods. Definitively, a more general approach to the segmentation of several significant tissue types (and not only the skin) is needed. For this purpose, in this paper an adaptive mean shift procedure for border-preserving region smoothing is used as a preliminary stage for region growing segmentation. The mean shift procedure has shown a high level of reliability in different image segmentation tasks.

Once the pressure ulcer images are segmented, a set of color and texture features is extracted from each resulting region. A principal component analysis (PCA) allows the reduction of dimensionality of the initial color and texture feature space. Finally, this pattern set is used to train supervised neural networks (multilayer perceptrons) and Bayesian classifiers, to categorize the tissue into five different tissue types: skin, healing, granulation, slough and necrosis.

The mean shift procedure can be considered a versatile tool for feature space analysis and can also provide reliable solutions for many vision tasks. In this study, we use the mean shift procedure for continuity-preserving smoothing of pressure ulcer digital images, as a previous critical stage to region segmentation.

Once the mean shift smoothing procedure has been applied, a region growing algorithm drives the image segmentation process. In the Fig. 12 given below, this region growing segmentation algorithm has been launched on an image which

is the result of the mean shift smoothing procedure. Segmented regions obtained this way are consistent with the separate areas of different significant tissues.

The main objective of this study is automatic tissue identification on wound images, to obtain a more effective tool for pressure ulcer clinical evaluation. To this end, we consider the issue of tissue recognition as the following categorization problem: the classification of each region from a segmented image as belonging to one tissue type.

Effectiveness results and examples on real pressure ulcer digital photographs have been presented, and the appropriateness of our proposed supervised approach for the efficient detection of significant wound areas has also been shown. The use of a Bayesian classifier to combine the classifications of the neural networks allows the efficient detection of particularly critical tissue, such as necrosis, which require invasive and immediate clinical intervention. The Bayesian-committee-machine approach provides better specificity scores than a more classical Ensemble-Averaged-Committee-Machine approach when classifying those tissues with low prevalence rates, such as necrosis, which is clinically a very desirable outcome.

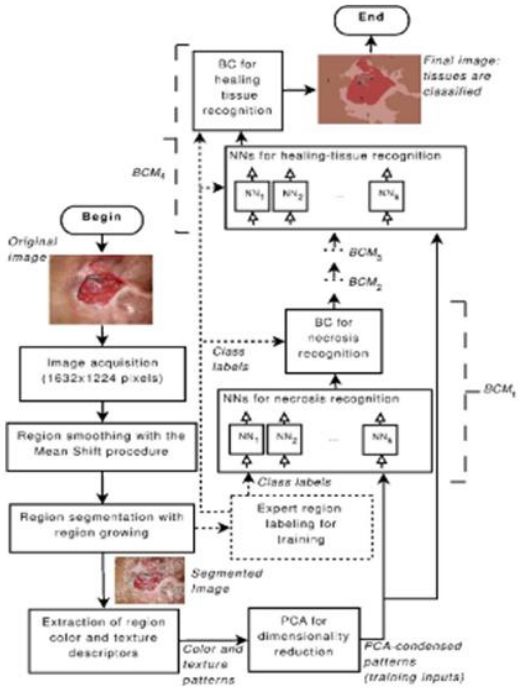

Fig. 11B. Flowchart for region segmentation and tissue identification on pressure ulcer digital images [28]

Fig. 12. In (A), a digital image of a typical pressure ulcer on a patient's sacrum is shown. In (B), the mean shift smoothing procedure has been applied to the image in (a). The image in (C) shows the results from the region-growing segmentation of the smoothed image in (b).

Now we are referring to the paper Detection and Analysis of Irregular Streaks in Dermoscopic Images of Skin Lesions [29]. Irregular streaks are important clues for Melanoma (a potentially fatal form of skin cancer). This paper extends our previous algorithm to identify the absence or presence of streaks in skin lesions, by further analyzing the appearance of detected streak lines, and performing a three-way classification for streaks, Absent, Regular, and Irregular, in a pigmented skin lesion. In addition, the directional pattern of detected lines is analyzed to extract their orientation features in order to detect the underlying pattern. The method uses a graphical representation to model the geometric pattern of valid streaks and the distribution and coverage of the structure.

Malignant melanoma, a form of skin cancer arising from the pigment-producing cells of the epidermis, is most treatable when the disease is diagnosed early. However, effective therapies for metastatic melanoma are lacking, and the five year survival rate is only 15% for the advanced stage. Fig. 13 shows examples of streaks.

Automating the recognition of streaks would help in building a computer-aided system for melanoma detection. Such a system would not only help physicians diagnose melanoma as a second reader, it could also teach the technique of dermoscopy. This paper presents a novel automated method, which builds upon and extends the earlier work This method analyzes the orientation and spatial arrangement of streak lines and classifies the lesion as a lesion with Absent, Regular, and Irregular streaks.

Peleg et al. [30] first proposed and outlined a method to detect streaks; they argued that the presence and absence of radial streaming and pseudopods and their characteristics could be tested from a skeleton of the pigment network. However, they did not publish the details of their algorithm. Betta et al. developed a method in which streaks were detected by simultaneously looking for occurrence of finger-like tracks along the contour of a lesion, and brown pigmentation for the corresponding region. Dividing an image into 16 sub-images, they computed, in each sub-image, the irregularity of the lesion border and also the hue component of the original color image in the HSV color space. The final diagnostic decision was made by a simple threshold on these computed values. The algorithm to locate streak lines is divided into four steps: preprocessing, blob detection, feature selection, and two-class classification.

This section describes the new contributions in this paper, analyzing streak orientation, feature extraction and classification.

The method for recognizing partial and complete radial streaming patterns builds upon and extends the earlier work [31,32], through identification of valid streak lines from the set of candidate streak lines, to reduce false positive streaks such as hairs and skin lines. The method also extends the analysis to identify the orientation and spatial arrangement of streak lines. These novel geometric features are used to identify not only the presence of streak lines, but whether or not they are Irregular or Regular; important for melanoma diagnosis.

Now we have to identify Valid Streak Lines from Candidate Streaks [33]. Skin lesions are mainly circular in dermoscopy images, but they can be any shape. The lesion shape is generalized as an ellipse that has the same normalized second central moment's as the lesion region. Two foci F1 and F2 are computed using the eccentricity of the ellipse. To test whether a line segment, for

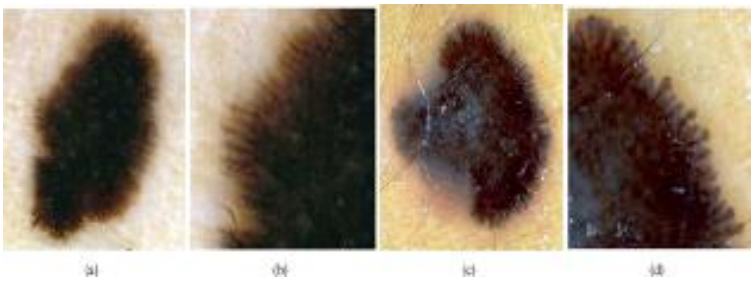

Fig. 13. Examples of streaks. Images (a) and (c) are lesions containing radial streaming and pseudopods pattern, respectively. Images (b) and (d) are magnified images to show the linear structures

example the red line segment with the angle β with respect to the horizontal direction and the centroid A1 of in Fig. 14(a), is a streak or not, A1 is connected to F1 and F2 and the angle between A1F1 and A1F2 is computed and its bisector line (A1B1) is found. It is expected that the orientation of a true streak line segment will coincide with the bisector line A1B1. To test such a condition, the angle between A1B1 and the line joining the Foci F1F2 ($\alpha 1$) is compared to the orientation angle ($\beta 1$) of the line. All orientations counterclockwise from the horizontal axis are measured in the range of [0, 2π]. By comparing $|\alpha - \beta|$ to a constant threshold of $\pi/6$, non-streak line segments are eliminated from the set of detected lines, and reliable line segments at every scale are found to form a multi-scale result to be used for feature extraction. Reliable lines detected after orientation enhancement are shown in Fig. 14(b), and the result of valid streaks selection is illustrated in the Fig. 14(c). These valid streaks are ordered in the direction of the red arrow from 0 to 2π for feature extraction in the next step.

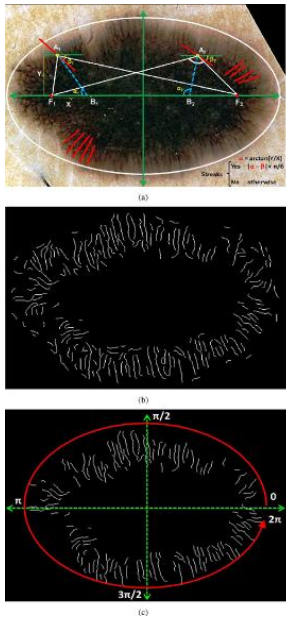

Fig. 14. Validating streaks candidates. Images (a) illustrates how line segments are filtered based on their orientation difference from the expected direction. Image (b) shows the line segments detected after orientation estimation and (c) shows valid streaks after removing false positives [29]

Based on the mathematical definitions of streaks proposed in [31], a new set of 18 features is proposed for streaks, called STR (streaks), which includes three Structural, three Geometric, six Orientation, and six Chromatic characteristics of valid streaks. Common color and texture features [34,35] of the lesion itself, called LCT (lesion color texture) has also been used.

LCT (Lesion color texture feature) includes the following 13 features: The mean, standard deviation and reciprocal of coefficient of variation (mean/stdev) of the values in S and V from HSV and L* of L*a*b*, and four of the classical texture measures; energy, contrast, correlation, and homogeneity [33,35]. These textural features are calculated from a grey level co-occurrence matrix (GLCM). The GLCM, constructed over the entire lesion, is a tabulation of how often different combinations of pixel brightness values (gray levels) occur in a pixel pair in an image.

The streak detection algorithm and the validation procedure outlined in the paper likely miss and/or exclude some “true” streak lines. In addition, the streak-specific features reported in Section III-B may not cover “all” streak properties. Thus the LCT feature set was constructed, in order to capture the “missing” information globally from the entire lesion. Potentially, the LCT set could include other dermoscopic features such as border asymmetry, irregularity and the color counts. However, the LCT set was restricted to the color and texture information that is more obviously useful for modeling streak patterns. In future, these streak features will be compared with other dermoscopic features to determine the predictive power of each of them.

These results demonstrate that the proposed approach can locate, visualize, and classify streaks as Absent, Regular, and Irregular in dermoscopy images. Therefore, it can be used in computer-aided melanoma diagnosis using scoring methods. Furthermore, since the proposed method locates streaks and provides a qualitative analysis, it can be used to highlight suspicious areas for experts’ diagnosis and for visualization and training purposes.

The method has been successfully applied in the specific case of automatic detection and classification of streaks, which are represented by linear radial patterns. Fig. 14 shows the results. These oriented patterns, produced by propagation, accretion, and deformation in radial phase, are common in nature and also in different fields of computer vision, and they are an important class for visual analysis.

Now we are referring to the paper Face Recognition using New Texture Representation of Face Images [36], Face recognition is substantially different from classical pattern recognition problems, such as object recognition. The shapes of the objects are usually different in an object recognition task, while in face recognition one always identifies objects with the same basic shape. This is of utmost difficulty for a face recognition system when one tries to discriminate faces all of which have the same shape with minor texture differences. The face recognition therefore depends heavily on the particular choice of face representation.

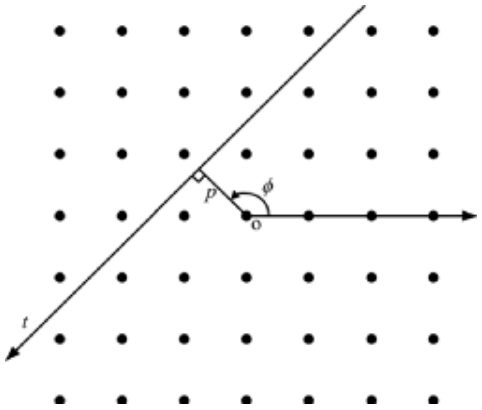

Fig. 15. Tracing line on an image with parameters (ϕ,ρ) and t

The Trace transform [37], a generalization of the Radon transform, is a new tool for image processing which can be used for recognizing objects under transformations, e.g. rotation, translation and scaling. To produce the Trace transform one computes a functional along tracing lines of an image. Each line is characterized by two parameters, namely its distance ρ from the centre of the axes and the orientation ϕ the normal to the line has with respect to the reference direction. In addition, we define parameter t along the line with its origin at the foot of the normal. The definitions of these three parameters are shown in figure below. The image is transformed to another image with the Trace transform which is a 2-D function depending on parameters (ϕ,ρ). Fig. 15 explains tracing a line on image with parameters.

The Trace transform is a global transform, applicable to full images. If we are going to use it to recognize faces, we must consider a local version of it. Having identified the faces in an image, we proceed here to define the masked Trace transform. The Trace transform is known to be able to pick up shape as well as texture characteristics of the object it is used to describe.

We show the result of the Trace transform of the full image, the rectangular face and elliptical shape in figure below. One can see that the inclusion of background sections destroys the local texture and structure of the Trace transform. However, with the masked Trace transform we can keep the local structure of the shape as well as texture characteristics. We therefore call this face representation the masked Trace transform (MTT). The values of the masked Trace transform may be regarded as some sort of “texture” characteristics of a face image.

In face recognition, one may have the problem of recognizing a face that is rotated, scaled and translated with respect to the face in the database. It can be seen that the masked Trace transform is shifted left or right by the corresponding amount of rotation. One can apply a matching algorithm on each column between original and rotated versions of the masked Trace transform.

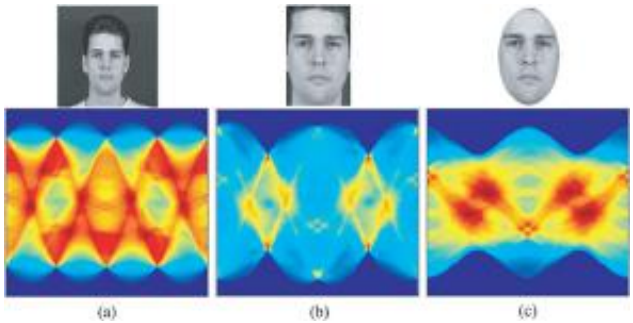

Fig. 16. Examples of the Trace transform. (a) Full image (b) rectangular shape and (c) elliptical shape

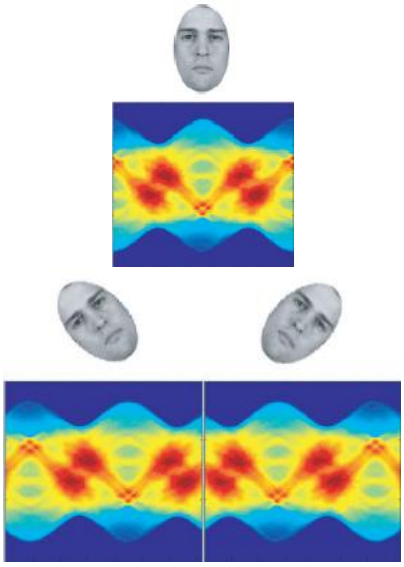

Fig. 17. An original face and its versions distorted by rotation. The corresponding masked Trace transform for each face version is shown in the bottom row

The masked Trace transform allows us the define a new way for face coding. We observe that there are subtle differences between the Trace transforms of different people that make them distinct, while the Trace transform of the same person seems to retain its structure over the three different images.

Every point in the Trace representation of an image represents a tracing line. Here, we shall describe a method for weighting each tracing line according to the role it plays in recognizing the face. We need to find the persistence of the features locally in the masked Trace transform for each person. So, by selecting the features in the Trace transform which persist for an individual, even when their expression changes, we are identifying those scanning lines that are most important in the definition of the person. Figs. 16 and 17 show the results.

In the paper Skin Detection using Contourlet Texture Analysis [38], an algorithm is proposed that combines color and texture information to segment skin regions in color images. Contourlet coefficients are used as texture features. Proposed method has training and test phases. In the training phase, these coefficients are classified by MLP. For test phase, at first the boosted pixel-based skin detection is used to characterize skin pixels from images. The used pixel-based skin detection is similar to our previous work in Texture features of skin-like region are extracted and recognized by MLP which decides between skin and non- skin regions. Then, a post-processing stage based on Markov property is applied to joint separate neighboring skin detected regions. In our approach, we assume a structure of classifiers that each of them is an explicit boundary skin detector in a specific color space. A boosting method called “unbiased voting” is used to combine the results of the classifier and makes a better final decision. This method gives a weight to each classifier. This weight indicates the effect of each classifier result in the final decision. The conducted experiments show a direct relation between true positive (TP) and false positive (FP) rates in skin detectors. We have found that if the classifier weights are determined in an order that a balance exists among high and low TP-FP classifier weights, the best results will be achieved. The pixel based boosted skin detector structure is shown in Fig. 16. The weight of each classifier is determined by (1) $w(i)=T(i)/\in T(j)$ where Ti is the TP rate of each explicit skin classifier on the training data. Threshold of pixel-based boosted skin detection is determined empirically to detect 95.2% of all skin-associated pixels and assessment then made in terms of the percentage of non-skin pixels incorrectly accepted. The lowest false acceptance rate found to be about 27.6%. The threshold can be change to achieve higher TP versus lower FP. The aim of our proposed method is to detect the early skin region with high TP and FP and then reduce the FP using texture analysis.

The contourlet transform can be employed as a texture representation method in two different settings. In the first case, patches of size 3232 are selected from the main image and their contourlet coefficients are calculated. In the second form, undecimated contourlet transform can be applied to the whole image and then the small patches are selected to process. The disadvantages of the first case are twofold; it needs a large patch size to apply the contourlet transform with high number of decomposition stages. In addition, if the minimum allowed patch size (i.e., 3232) is used, the final skin map will have low quality due to the fact that skin pixels on the object borders are detected as non-skin. This will be as a side effect of limited locality of the algorithm. However, in the second case the patch size can be changed freely to tune the locality of the method. Hence, the second form of texture representation will be used with 8 and 16 directions decomposition in the first and second stage, respectively. To train the system a set of 300 color images are selected. Each image pixels are labeled in prior either as a skin or non-skin pixel. A basic color-based skin detector is employed to extract skin candidate pixels of these images. Those candidate pixels that are labeled in prior by the user as skin or non-skin, are considered as positive and negative samples, respectively. In order to further process the skin colored pixels, the color representation of the main image is changed to YCbCr format.

In this system the color information is separated from intensity. The texture of the local area around each skin colored pixel can be extracted from the Y component. In fact, the proposed method tries to model the nonskin pixels that have skin color and cannot be detected using the color-based skin detector. To model these cases successfully, the texture feature of pixels is needed. In contrast with non-skin areas, the local texture content of the skin pixels usually varies smoothly. Contourlet transform proves to be a suitable candidate for texture classification, since it decomposes the input image in frequency domain into different directions. Therefore, for each sample pixel, a patch of size 5by5 around that pixel in all sub images is used as the local texture feature. Then, each patch matrix will be row-ordered to get the features in the vector form. The PCA transform of the vector samples is used, since the contourlet coefficients are highly redundant. Analyzing the eigenvalues, it is found that using 70 first PCA coefficients, at least %95 of the total signal energy will be preserved. Finally, to classify the samples, an artificial neural network is used. The skin and non-skin class target value is considered as +1 and -1, respectively. In the test phase, the contourlet transform of the whole test image is first computed. Then, the basic color-based skin detector is used. For candidate skin pixels, the set of 55 patches around that pixel in all sub images are selected and projected in the trained PCA subspace to get the 70 topmost dimensions. The 70 features are then fed into the trained neural network. The label of the pixel can be determined according to the sign of the network output.

Using 300 skin images, 3500 positive and negative training data were extracted and used to train a MLP with two layers of 14 and 9 neurons. Classification was performed using the sign of the network output. In color-based skin detection, RGB, YCbCr, HSV, Nrgb, and YIQ color space were used. In the post processing stage, if 65% of pixels in a block were detected as skin, the block center was also marked as skin. The proposed method was tested on a number of images. Fig. 18 shows the result of the algorithm.

In this paper, the advantage of the texture information is taken in addition to color feature to devise a skin detection algorithm. Nonsubsampled contourlet transform was proved to be a suitable texture. A learning classifier was employed to perform texture classification of pixels. Additionally, the Markov property of natural images is employed to join separate skin detected regions. The proposed configuration shows significant improvement on false positive rate with respect to one of the state-of-the-art methods based on texture information.

In the paper, An efficient algorithm for fractal analysis of texture [39], where a completely new texture feature extraction method is proposed, which is named as the segmentation based fractal texture analysis method. The proposed method basically decompose the input image into a set of binary images and then the fractal dimensions of the resulting regions are computed so that the segmented texture pattern can be classified.

The purpose of this paper is firstly to decompose the input images into a set of binary images by the two threshold binary decomposition algorithm and to evaluate the STFA for image classification and for the tasks of content based image retrieval and to compare the performance of this

STFA method with the already existing extraction method.

The STFA algorithm is broadly categorized into two main parts. (i) Usage of the TTBD (Two-threshold binary decomposition) technique method for the conversion of input gray scale image into binary images. (ii) Then for each resulting binary image fractal dimensions, mean gray level, and size are calculated.

(i) The threshold binary decomposition method is as follows – firstly it computes a set of threshold values. This set of the threshold values is obtained by selecting equally spaced gray level values. Next the authors had the decomposition of input gray scale images I(x,y) into the binary images is achieved by selecting pairs of thresholds from T and then the two threshold segmentation is followed by I(x,y)=1 if t(l) <I(x,y)<t(u) and I(x,y)=0 otherwise. where the t(l) and t(u) are the upper and lower threshold values. The following figure illustrates the method of the TTBD (two threshold binary decomposition) in brief.

(ii) STFA feature extraction algorithm is as follows. After applying the TTBD to the input gray level image the STFA feature vector is obtained from the set of the threshold values obtained from the multilevel otsu algorithm. Thus the feature vector is constructed as the resulting binary image size, mean gray level, and boundaries fractal dimension. The fractal measurements are calculated or computed in order to describe the complexity of the objects and the structures segmented in the input image. Thus the STFA feature vector corresponds to the number of images obtained by the TTBD multiplied by three because the following measurements like area, mean gray level, and fractal dimension is calculated. The following two Figs. 19A and 19B pictorically represents the STFA algorithm as proposed in the paper.

First the input image is decomposed into a set of the binary images by the TTBD algorithm. Then the STFA feature vector is constructed as the resulting binary image's size, mean gray level and boundaries fractal dimension [39].

A_1 = Area, $\bar{u}_1$ = Mean, D_1 = Fractal Dimension

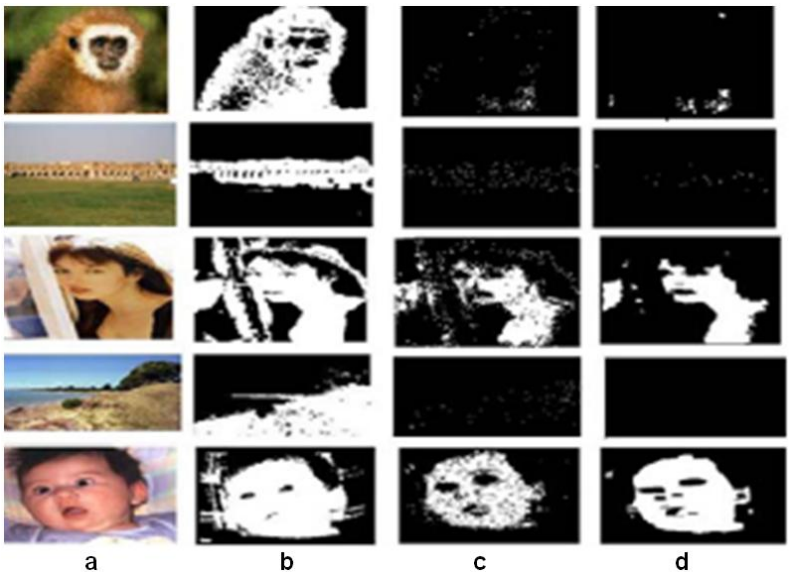

Fig. 18. Results of applying nonsubsampled contourlet transform on whole image with post-processing. (a)Original image, (b) boosted pixel-based skin detection, Input Image Y Color-based skin detection changing to YCbCr space Contourlet Transformation based on Y Component Selecting 5×5 Patches Around Skin-Colored Pixels Row-Ordering Patch Coefficients in each Subimage Coefficient Concatenation ANN Classifier Decision on Pixel (a) (b) (c) (d) classification of pixels with contourlet features, (d) post-processed results

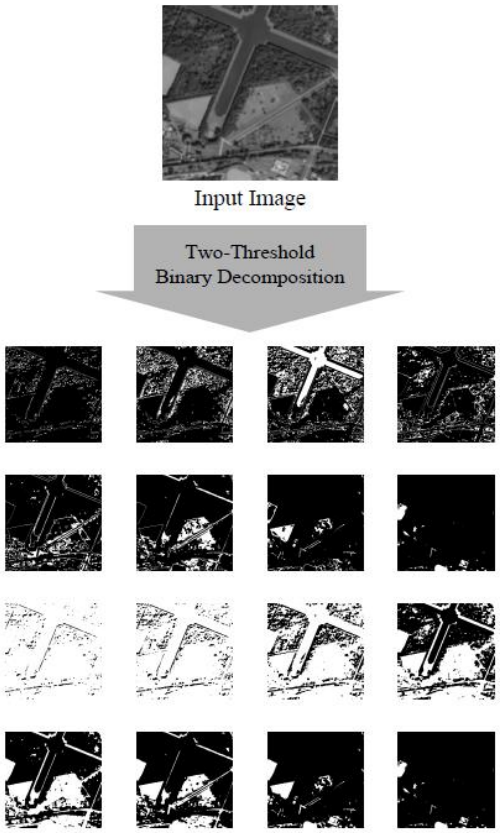

Fig. 19A. Decomposition of the region taken from the satellite images using the TTBD algorithm [39]

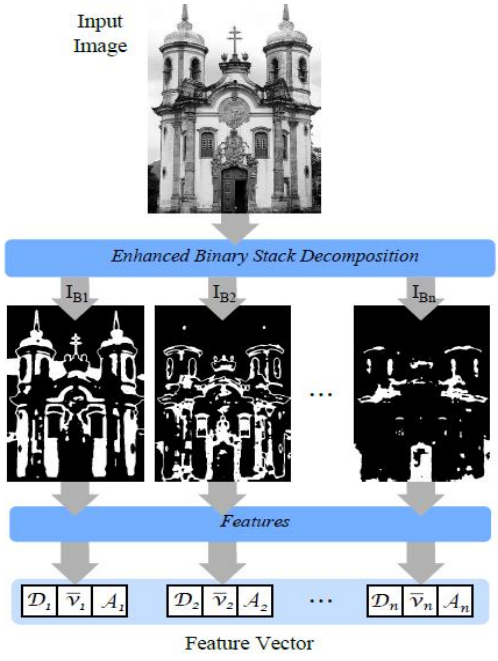

Fig. 19B. STFA extraction diagram taking an input gray scale image

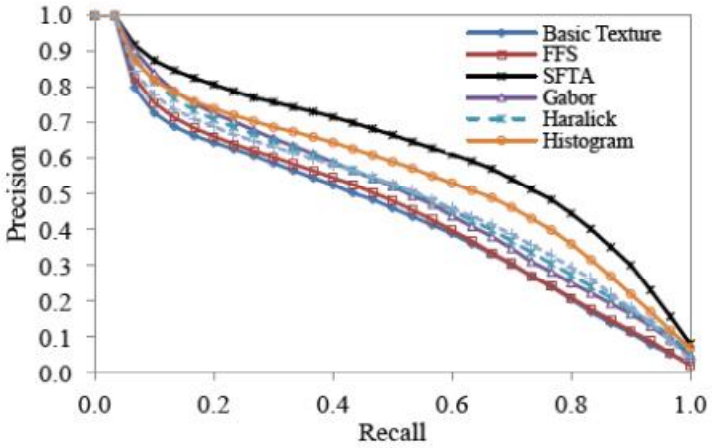

Fig. 19C. Precision and recall curves is obtained for the lung CT ROIs dataset and STFA presenting the highest image retrieval precision for all recall curves [39]

SFTA algorithm is compared with the widely known feature extraction method like Haralick descriptor, gabor filter banks and others on the basis of the image classification accuracy and CBIR precision. STFA is proved to be 3.7 times faster than Gabor and 1.7 times faster than Harlick descriptor on the basis of the feature extraction time. The analysis is shown in Fig. 19B.

5. CONCLUSION

In this paper we have discussed about what is digital image processing, texture recognition and discussed briefly about the prior recent work, but the aim of the paper is to criticize the technological gap and to highlight the problem area faced in the field of texture recognition. A large number of papers across the different technologies that are used for texture analysis that varies from fractal to artificial neural network to statistical models and others had been surveyed and found that each technology has their pros and cons. We had shortlisted the best and most recent papers studied in each technology and presented their review in our paper. The advantages and shortcomings of the paper are discussed in our paper. Since, the papers studied varies in technologies, so no generic comparison is done but individual analysis of the papers are done.

COMPETING INTERESTS

Authors have declared that no competing interests exist.

REFERENCES

1. Acharya T, Roy AK, Image processing principles and applications, Wiley Publication; 2005.
2. Christophe Garcia, Georgios Tziritas. Face detection using quantized skin color regions merging and wavelet packet analysis. IEEE Transactions on Multimedia. 1999;1(3).
3. Gholamreza Akbarizadeh. A New recognition approach based on genetic algorithm for classifying textures in satellite SAR images. Electrical Engineering Department, Engineering Faculty, Shahid Chamran University of Ahvaz (SCU), Ahvaz
4. Julesz B. Experiments in the visual perception of textures. Scientific America. 1975;232:34-43.
5. Julesz B. A theory of pre-attentive texture discrimination based on first order statistics of textons. Biol. Cybernet. 1981;41:131-138.
6. Conners RW, Harlow CA. A theoretical comparison of texture algorithms. IEEE Transactions on Systems Man and Cybernetics. 1991;21(I):252-261.
7. Dyer CR, Hong TH, Rosenfield A. Texture classification using gray level co-occurrence based on edge maxima. IEEE Transactions on Systems, Man. and Cybernetics. 1980;10:158-163.
8. Zucker SW, Terzopoulous D. Finding structure in co-occurrence matrices for texture analysis. Computer Graphics and Image Processing. 1980;12:286-308.

9. Jawahar CV, Ray AK. Incorporation of gray level imprecision in representation and processing of digital images. Pattern Recognition Letters. 1996;17:541-546.
10. Davis LS, Johns SA, Aggarwal JK. Texture analysis using generalized co-occurrence matrices. IEEE Trans. Putt. Anal. Mach. Intell., PAMI-1(3). 1979;251-259.
11. He DC, Wang L. Texture unit, texture spectrum and texture analysis. IEEE Trans. Geoscience and Remote Sensing. 1990;8(4):509-512.
12. He DC, UJang L. Texture features based on texture spectrum. Pattern Recognition. 1991;24:391-399.
13. He DC, Wang L. Unsupervised textural classification of images using the texture spectrum. Pattern Recognition. Texture and Shape Analysis. 1992;25(6):247-255, 206.
14. Mandelbrot B. The Fractal Geometry of Nature, Freeman Co., San Francisco; 1982.
15. Pentland AP. Fractal based description of natural scenes. IEEE Trans. on Pattern Analysis and Machine Intelligence. 1984;6: 661-674.
16. Bhattacharya R, Patrangenaru V. Large sample theory of Intrinsic and extrinsic sample means on manifolds. Ann. Statistics. 2003;31:1-37.
17. Srivastava A, Joshi SH, Mio W, Liu X. Statistical shape analysis: Clustering, learning, and testing. IEEE Trans. on Pattern Analysis and Machine Intelligence, PAMI-27(4). 2005;590-602.
18. Kent JT, Mardia KV. Procrustes tangent projections and bilateral symmetry. Biometrica. 2001;88:469-485.
19. Teh CH, Chin RT. On the detection of dominant points on digital curves. IEEE Trans of Pattern Anal. and Machine Intel. 1989;11(8).
20. Kass HL, Witkin A, Terzopoulos D. Snakes: Active Contour Models, Proceedings of First International Conference on Computer Vision, London. 1987;259-269.
21. Xu C, Prince JL. Snakes, shapes and gradient vector flow. IEEE Trans. on Image Processing. 1998;7(3).
22. Celebi ME, Aslandogan YA. A comparative study of three moment-based shape descriptors. Proc. of the IEEE International Conference on Information Technology: Coding and Computing, Las Vegas, NV; 2005.
23. Persoon E, Fu K-S. Shape discrimination using fourier descriptors. IEEE Trans. On Systems, Man and Cybernetics, SMC-7(3). 1977;170-179.
24. Jason M Kinser, Guisong Wang. Texture recognition of medical images with the ICM method. Elsevier Journal Nuclear Instruments and Methods in Physics Research A. 2004;525:387–391.
25. Oana G Cula, Kristin J Dana, Frank P Murphy, Babar K Rao. Bidirectional imaging and modeling of skin texture. IEEE Transactions on Biomedical Engineering. 2004;51(12).
26. NIdhal K ALabdadi, NAzir saadi Dhur, Zaid Abd ALkareem. Skin texture recognition using neural networks, IT research and development Cetre, Kufa University.
27. Silvio M Pereira, Marco AC Frade, Rangaraj M Rangayyan, Paulo M Azevedo-Marques. Classification of color images of dermatological ulcers. IEEE Journal of Biomedical and Health Informatics. 2013;17(1).
28. Francisco Veredas, Héctor Mesa, Laura Morente. Binary tissue classification on wound images with neural networks and bayesian classifiers. IEEE Transactions on Medical Imaging. 2010;29(2).
29. Maryam Sadeghi, Tim K Lee, David McLean, Harvey Lui, Stella Atkins M. Detection and analysis of irregular streaks in dermoscopic images of skin lesions. IEEE Transactions on Medical Imaging. 2013;32(5).
30. Peleg S, Naor J, Hartley R, Avnir D. Multiple resolution texture analysis and classification. IEEE Trans. on Pattern Analysis and Machine Intelligence, PAMI-6(4). 1994;518-523.
31. Julesz B. Visual texture discrimination. IRE Trans. On Inf. Theory. 1962;8:84-92.
32. Julesz B, Gilbert EN, Shepp LA, Frisch HL. Inability of humans to discriminate between visual textures that agree in second-order statistics –revisited. Perception. 1973;2: 391-405.
33. Leu J-G. Shape normalization through compacting. Pattern Recognition Letters. 1989;10:243-253.
34. Williams DJ, Shah M. A fast algorithm for active contours and curvature estimation. CVGIP: Image Understanding. 1992;55(1): 14-26.

35. Haralick RM, Shanmugam K, Dinstein I. Textural features for image classification, IEEE Trans. Syst. Man Cybern., SMC-3. 1973;610-621.
36. Sanun Srisuk, Kongnat Ratanarangsank, Werasak Kurutach, Sahatsawat Waraklang. Face recognition using a new texture representation of face images. Advanced Machine Intelligence Research Laboratory (AMIRL) Department of Computer Engineering Department of Information Technology Mahanakorn University of Technology, Bangkok, THAILAND.
37. Gonzalez RC, Woods RE, Digital image processing. Pearson Education India; 2009.
38. Mehran Fotouhi, Mohammad H Rohban, Shohreh Kasaei. Skin detection using contourlet texture analysis. Sharif University of Technology, Computer Engineering Dep., Tehran, Iran; 2009.
39. Alceu Ferraz Costa, Gabriel Humpire-Mamani, Agma Juci Machado Traina. An efficient algorithm for fractal analysis of textures. Conference on Graphics, Patterns and Images (SIBGRAPI). 2012;39-46.

Peer-review history:
The peer review history for this paper can be accessed here:
http://sciencedomain.org/review-history/12759